المجلة العراقية للبحوث الإنسانية والإجتماعية والعلمية
Iraqi Journal of Humanitarian, Social and Scientific Research
Print ISSN 2710-0952 Electronic ISSN 2790-1254
العـــدد 17 أيـار 2025
No.17 May 2025

دراسة تأثير ليزر النبضة على الخواص البصرية والتركيبية لأغشية أشباه الموصلات العضوية الرقيقة P3HT

فالح لفتة مطر
rasha.m.saray.phys598@st.tu.edu.iq
رشا مزاحم ساري
جامعة تكريت- كلية العلوم – قسم الفيزياء.
[2]البريد الالكتروني: Faleh.l.mater@tu.edu.iq

١. الملخص

تجعل الخصائص الفريدة لأشباه الموصلات العضوية منها واحدة من أهم المواد وأكثرها فائدةً في تطبيقات أشباه الموصلات. صُنعت عينات من أشباه الموصلات العضوية (P3HT) وفُحصت وقُيّمت خصائصها البصرية قبل تشعيعها بالليزر النبضي. وشملت الأجهزة المستخدمة: الأشعة فوق البنفسجية (UV)، وتقنية الأشعة السينية (XRD)، وتقنية تحويل فوريه للأشعة تحت الحمراء (FTIR)، وتقنية المجهر الإلكتروني الذري (AFM). بعد تعريض المادة (P3HT) لشعاع ليزر، أُعيد تقييم خصائصها البصرية. لمدة ١٥ ثانية، استُخدم ليزر Nd:YAG نبضي بطول موجي ٣٥٥ نانومتر وبتردد تكرار ثابت ٥ هرتز، مع طاقات ليزر نبضية متفاوتة تبدأ من (١٥٠)، و(٢٥٠)، و(٣٥٠)، و(٤٥٠) مللي جول على التوالي. كان الهدف الرئيسي لهذا البحث هو تقليل قيمة فجوة الطاقة للجزيء العضوي المُشعع. وبالتالي، ستُسهّل المواد العضوية نقل الإلكترونات عبر مستويات طاقة مختلفة مع تقليل كمية الطاقة المطلوبة. تُعد الثنائيات العضوية الباعثة للضوء (OLEDs)، وهي بديل لثنائيات OLED التقليدية، أحد الاستخدامات العديدة التي تتيحها كمية الإلكترونات المثارة بين المستويين، مما يزيد بدوره من عدد الفوتونات المنبعثة.

الكلمات المفتاحية: مادة اشباه الموصلات العضوية P3HT، ليزر النبضات، فجوة الطاقة ، تطبيقات اشباه الموصلات.

Study the impact of Pulse laser on the Optical and Structural Properties of P3HT Organic Semiconductor thin Film

Rasha Mozahem Sari[1] & Faleh Lafta Mater[2]
1,2 Tikrit University - College of Science - Department of Physics
[1]Corresesponding auhor Email: rasha.m.saray.phys598@st.tu.edu.iq
[2]Email Adress: Faleh.l.mater@tu.edu.iq

1. Abstract

The unique characteristics of organic semiconductors make them one of the most essential and potentially useful materials for semiconductor applications. Organic semiconductor (P3HT) samples were manufactured, inspected, and evaluated for optical characteristics prior to irradiation with a pulsed laser. The instruments that were utilized were (UV), (XRD), (FTIR), and (AFM). After subjecting the material (P3HT) to a laser beam, its optical characteristics were reevaluated. For 15 seconds, a pulsed Nd:YAG laser with a wavelength of 355 nm and a constant repetition rate of 5 Hz was employed, with varying pulse laser energies beginning at (150), (250), (350), and (450)mJ, respectively. Pursuing a decrease in the energy gap value of the irradiated organic molecule

was the primary objective of this research. Consequently, organic materials will make it easier to move electrons across different energy levels while also reducing the amount of energy required. Organic light-emitting diodes (OLEDs), a substitute for conventional OLEDs, are one of many uses made possible by the quantity of excited electrons between the two levels, which in turn increases the number of photons emitted.

Keywords: Organic semiconductors material (P3HT), Pulse laser, Energy gap, semiconductor applications.

2. **Introduction**

Germanium (Ge) and silicon (Si) are necessary components for electronic devices that use inorganic semiconductors. On the other hand, they are susceptible to a number of constraints, including as their hefty weight, high production costs, and restricted flexibility in comparison to organic semiconductors. Because of this, progress in the study of organic semiconductors can offer an alternative way to get around these problems in the field of electronic materials. These improvements can provide good and useful ways to solve these problems and pave the way for a new generation of electronics [1]. The unique electrical applications that organic semiconductors may give, which are not possible with conventional crystalline inorganic semiconductors, have led to their fast growth in recent years. The fundamental differentiating characteristics of these materials provide them important alternatives to inorganic semiconductors [2-5]. For instance, the molecular structure of organic semiconductors can be accurately controlled, they are lightweight and flexible, they can be produced at low temperatures, they have low process costs and solution capabilities, and their optoelectronic properties can be customized [6-8]. Thin film deposition on various surfaces, mechanical flexibility, transparency, and the use of eco-friendly ingredients are just a few of the many benefits of organic semiconductors. Various optical and electrical devices and systems are among the many uses [9-10]. Thin film devices are able to work at their peak efficiency when organic solar cells' electrical arrangement is optimized. In organic photovoltaic devices (OPVs), for instance, the dissociation of photoexcited charges is impacted by the energy level variations between the lowest unoccupied molecular orbital (LUMO) and the highest occupied molecular orbital (HOMO) [11]. Biomedical sensors, thin-film organic solar cells, image sensors, flexible microprocessing, organic light-emitting diode displays, photovoltaics, and organic photovoltaics devices are just a few of the many uses for organic semiconductors, which offer a number of benefits over their inorganic counterparts [12-15].

3. Experimental Methods

Poly [3-Hexyl Thiophene] (P3HT) is a 99% pure organic polymer with a low molecular weight and belongs to the polythiophene family. Acquired from Ossila Co., Ltd. One component of organic solar cells is P3HT which is an organic semiconductor of the P-type. Due to its unique characteristics, cheap cost, and ease of production, P3HT is considered one of the best conductive polymer materials. Due to its high crystalline, excellent thermal stability, high charge mobility, environmental stability, and light-absorbing properties, as well as its solubility in a variety of organic solvents, such material is the most widely used polymer for organic optoelectronic applications, solar cells and photovoltaic devices. P3HT is a potential material for the creation of laser active medium and has been employed extensively in the development of OLEDs [16-20]. In Figure 1 it can be seen the P3HT molecular structure.

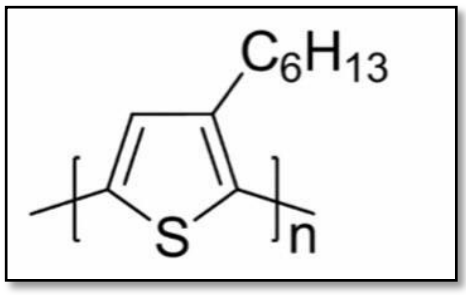

Figure 1. Chemical Structure of Poly(3-hexylthiophene) (P3HT)

This work successfully coated organic P3HT films onto glass substrates using the spin casting procedure. Using a concentration of 40 mg/ml, P3HT was dissolved in dichlorobenzene for solution preparation. Using a spin speed of 3500 rpm, thin films were produced. The prepared samples were exposed to A Nd-YAG pulse laser with a wavelength of 355 nm with different energy values ranging between 150, 250, 350, and 450 mJ, with a fixed exposure time of 15 seconds, and frequency of 5 Hz. The absorption, reflection, and transmission spectra, as well as other optical characteristics, of both the main and irradiation P3HT film samples were studied using a spectrophotometer that covered the ultraviolet to near-infrared spectrum. By analysing the absorption and transmission spectra of the molecules involved in chemical processes, FTIR was used to study the molecular fingerprint, which allowed researchers to analyse the organic molecule thin film's chemical composition and identify the presence of certain functional groups. The morphology and surface roughness of the samples were examined using an Atomic Force Microscope (AFM) both before and after laser irradiation. Finally, the crystalline structure of the samples was studied using XRD both before and after laser irradiation.

4. Results and Discussion

4.1 Optical absorption and coefficient of optical absorption

Figure 2 displays the time-dependent absorbance spectra of deposited and irradiated P3HT thin films. A wide absorption band at a maximum wavelength of 550 nm with an intensity of up to 0.9 was seen in the absorption spectra of a film that had been previously prepared. One key indication of the nature of molecular electronic transitions is the absorption in the visible light region, which is thought to be caused by electronic transitions caused by the excitation of non-bonding electrons. A red shift in the absorption edge towards higher wavelengths was detected when comparing this spectrum with the film's spectra before irradiation. This shift indicates that the electronic structure changed as a result of irradiation. Results showed that at various irradiation energies of 450, 350, 250, and 150 mJ, the absorption intensity increased progressively with increasing laser beam energy, reaching values of 0.9, 1.52, 0.63, and 0.51, respectively. This research primarily focuses on the greatest absorption intensity value of 1.52 with irradiation energy of 350 mJ. On the other hand, a drop in intensity was noted when the irradiation energy was raised to 450 mJ, suggesting that the material may experience damaging effects or saturation in its absorption at such high energies.

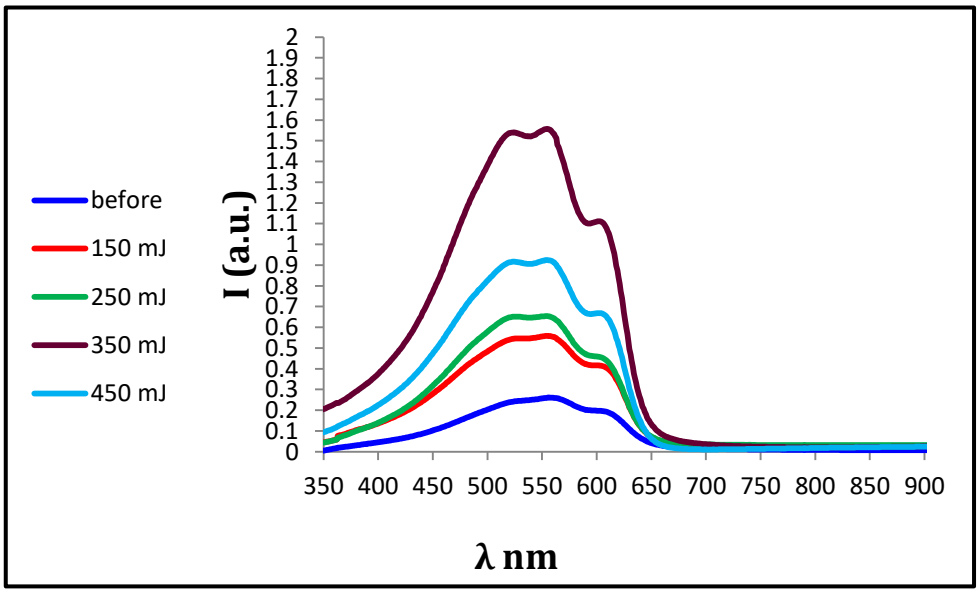

Figure 2.

Illustrates a comparison of the absorption spectra of P3HT thin films exposed to radiation and those that were deposited at various periods

The absorption spectra of P3HT thin films both beforehand and after irradiation using pulse laser with energy of (350 mJ), where the focus of the study are displayed in Figure 3. At around 550 nm, the untreated P3HT film shows a clear absorption edge. Following radiation, the absorption spectra show two distinct peaks at 550 and 520 nm, with the absorption strength in the visible region being much higher than in the near-infrared or ultraviolet regions. The

conjugated chain of the P3HT polymer backbone is responsible for the two peaks, one at 520 nm (2.38 eV) and the other at 550 nm (2.25 eV), which are attributed to π-π^* electronic transitions. There is an extra shoulder peak at 600 nm, which is probably associated with the piling up of P3HT molecules; this suggests that the film's crystalline order and regularity have improved. The energy gap has decreased due to molecule structural rearrangement, as shown by the red shift in the absorption spectra. Pulsed laser treatment causes a dramatic rise in absorption intensity because the polymer chains undergo direct bond breakage **[21]**.

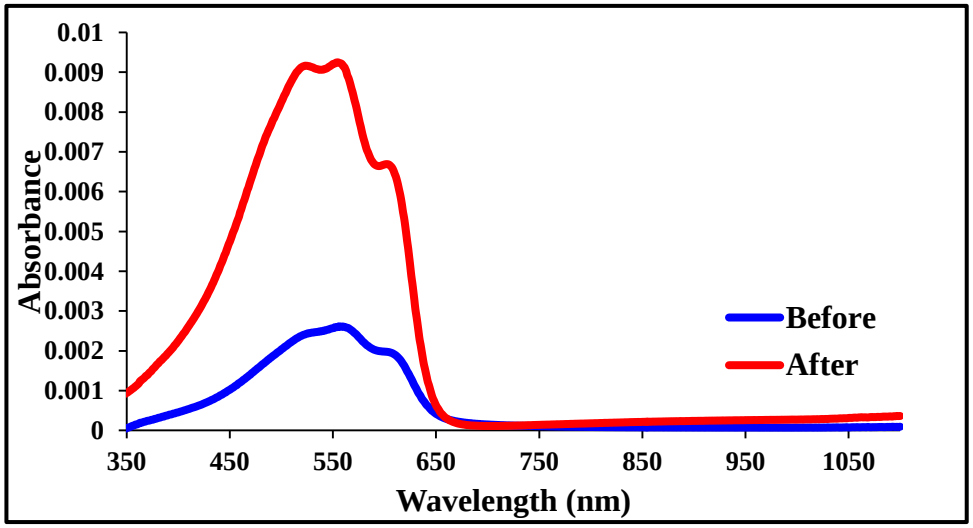

Figure 3. Displays The P3HT thin films' absorption spectra both before and after with pulsed laser beams of energy (350 mJ).

Based on the transmittance values, the optical absorption coefficients of the samples are determined using Equation 1 [22]:

$$\alpha = \frac{1}{d}\ln\left[\frac{(1-R)^2}{2T} + \sqrt{\frac{(1-R)^4}{4T^2} + R^2}\right] \quad \text{..... (1)}$$

The variables α, d, T, and R are refer to the absorption coefficient, thickness of the thin films, and reflectance and transmittance, respectively. Both the untreated P3HT thin film and another one that was exposed with pulse laser using energy of (350 mJ) have their absorption coefficients displayed in Figure 4.

A significant improvement in the absorption coefficient of the samples was observed after pulse laser treatment. This improvement in absorption in the visible range is attributed to a decrease in C=S, C–H, and C=C bonds, as a result

of exposing the samples to laser radiation in air, which led to chemical changes in the surface structure.

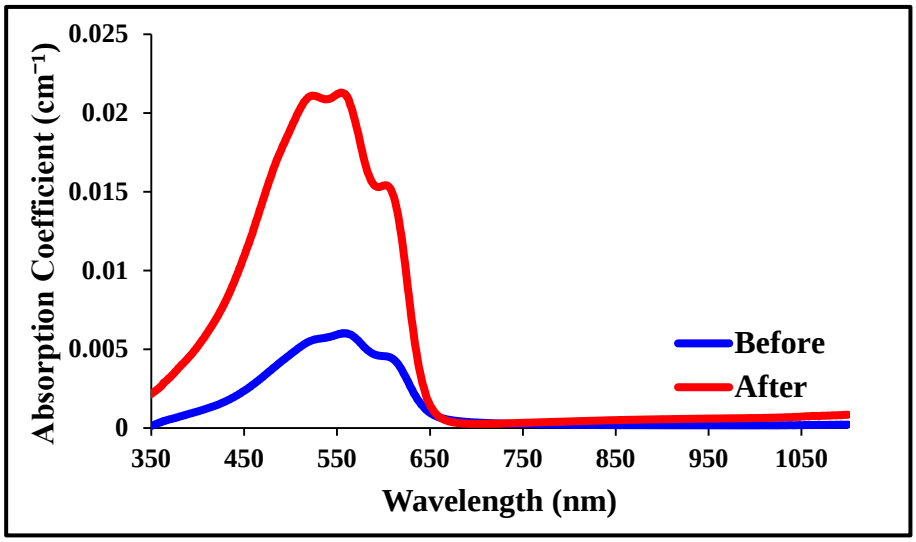

4. Figure Shows absorption coefficient curves of P3HT thin films before and after irradiation with pulsed laser beams of energy (350 mJ).

The absorption coefficient (α) is an indicator of the efficiency of the films in absorbing light. The nature of the electronic transitions can be identified by knowing the absorption coefficient. It is clear that the absorption coefficient increases as a result of increasing absorbance values.

4.2 The spectrum of transmittance and reflectance

The transmittance (T) can be determined by calculating the transmittance-wavelength relationship for polyhexylthiophene (P3HT) films. Figure 5-a shows the light transmittance (T) of the deposited P3HT films irradiated with a pulsed laser at an energy of 350 mJ. The changes in the transmittance spectrum are interpreted as resulting from the change in surface roughness of the samples after pulse laser treatment. It is also noted that P3HT has a high light transmittance in the spectral range above $\lambda > 400$, and the high absorption in the range between 400 and 650 nm is attributed to the decrease in the energy gap. The significant decrease in transmittance in the range $\lambda < 650$ nm may be due to the partial decomposition of P3HT by laser irradiation at an energy of 350 mJ, which clearly affected its optical properties.

Figure 5-b illustrates the relationship between reflectivity and wavelength for Polyhexylthiophene (P3HT) before and after laser exposure with an energy of 350 mJ. The graph shows that the reflectivity before exposure was relatively low across the studied wavelengths, while it increased significantly after laser exposure, particularly in the range between 400–650 nm. A prominent reflectivity peak was observed at a wavelength of approximately 550 nm after irradiation, indicating changes in the molecular structure or surface structure of

the film as a result of the absorption of laser energy. This increase in reflectivity can be explained by the stimulation of molecular rearrangements or changes in surface roughness, which increased the film's ability to reflect light within this spectral range. The increased reflectivity is also attributed to increased material density, resulting from bond changes and restructuring using the pulsed laser [23].

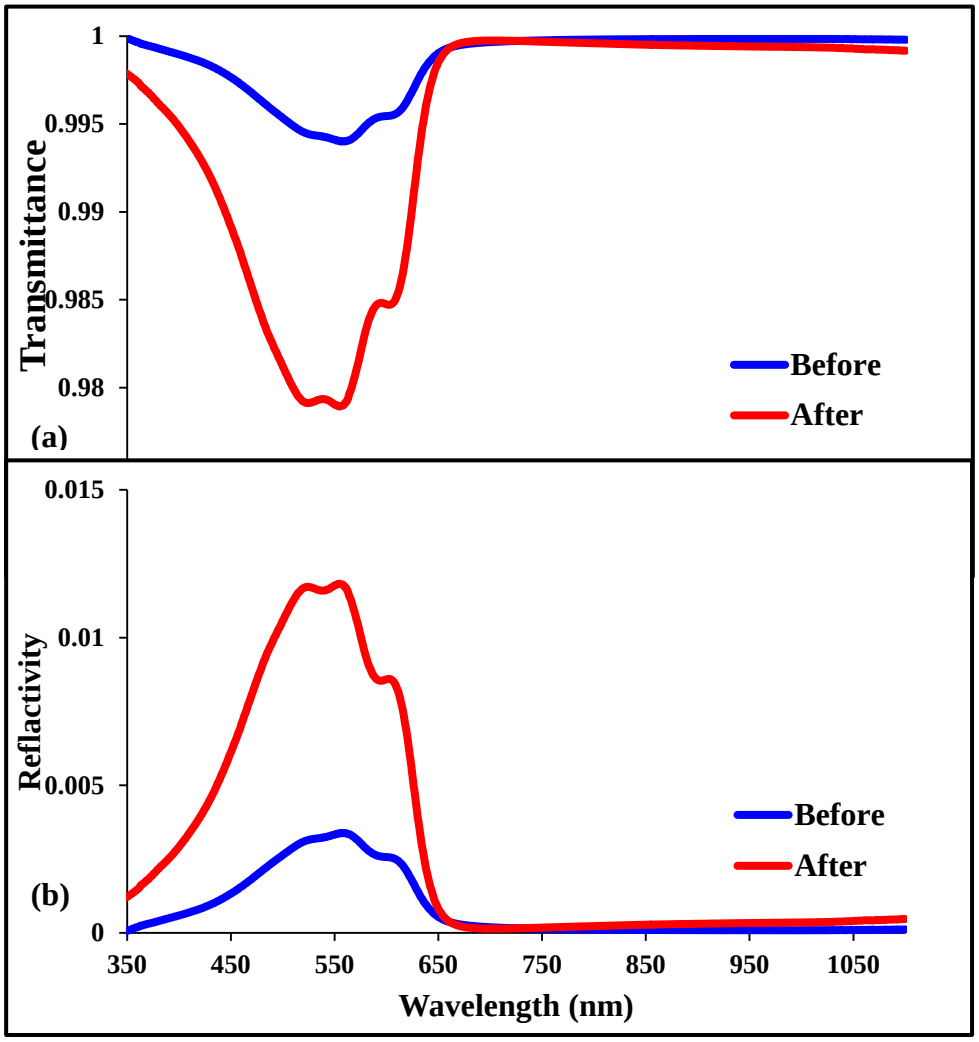

Figure 5. Illustrates (a) The optical transmittance T and (b) reflectance R of P3HT film and for another P3HT thin film irradiation with pulsed laser beams of energy (350 mJ).

4.3 Refractive index and extinction coefficient

The refractive index (n) and extinction coefficient (k) as functions of wavelength are illustrated in Figures 6 and 7, respectively. The extinction coefficient (k) and refractive index (n) clearly increased after laser treatments.

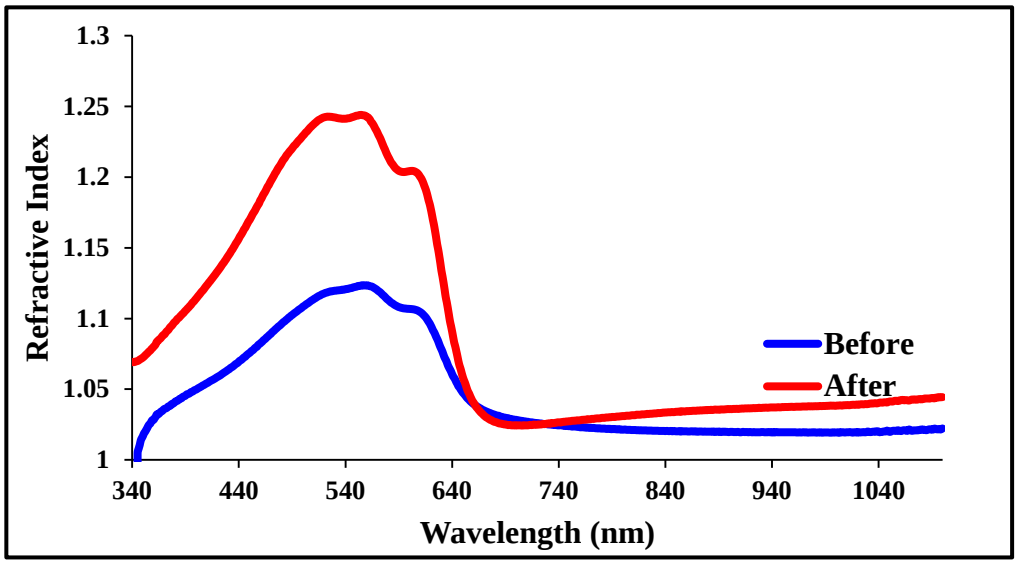

Figure 6. The refractive index (n) of P3HT film and for another P3HT thin film irradiation with pulsed laser beams of energy (350 mJ).

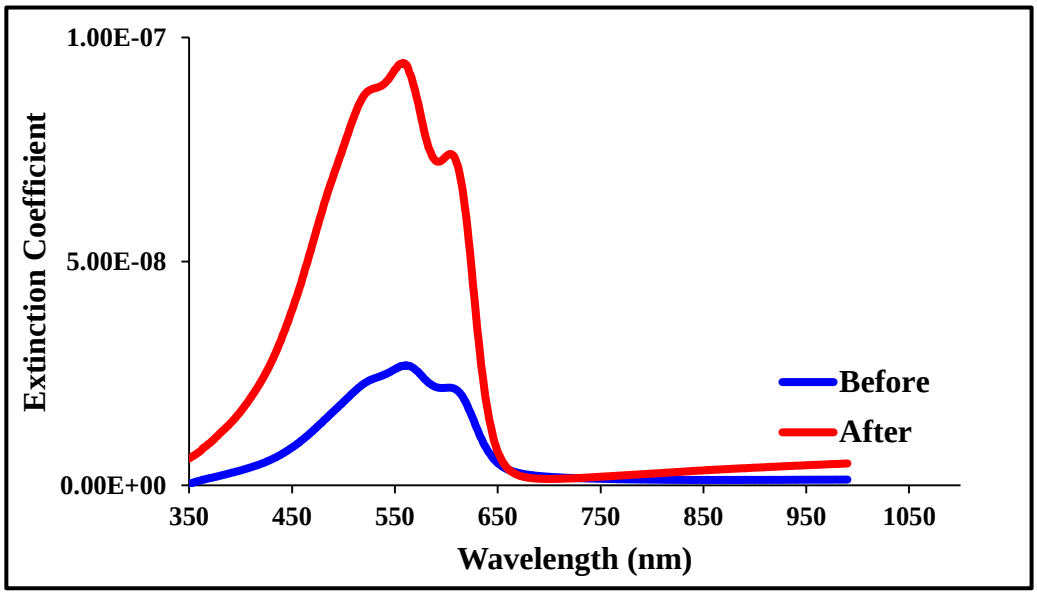

Figure 7. The extinction coefficient (k) of P3HT film and for another P3HT thin film irradiation with pulsed laser beams of energy (350 mJ).

The refractive index (n) is shown in Figure 6 as a function of wavelength for Polyhexylthiophene (P3HT) films before and after irradiation using pulsed laser beams of energy (350 mJ). It is evident that after laser treatment, the refractive index also increases. This change is attributed to the higher absorption coefficient of the treated samples. The refractive index value increases after irradiation until it reaches its highest value (1.24) at 350 mJ of energy,

compared to its pre-irradiation value of (1.11). Carbon-carbon bond polarization is another possible explanation for the observed change in the refractive index. These phenomena lead to interactions at the interphase level, resulting in rearrangement of the polymer chains and stimulating photochemical reactions on the surface of the P3HT material.

When studying the optical characteristics of materials, it is important to use equation 2 below to find the optical constants n and k:

$$\boldsymbol{n = \left(\frac{1+R}{1-R}\right) + \sqrt{\frac{4R}{(1-R)^2} - \quad k^2}} \text{.....(2)}$$

in which $\boldsymbol{k = \frac{\alpha\lambda}{4\pi}}$

Figure 7 shows the relationship between the extinction coefficient (K) and the wavelength of polyhexylthiophene (P3HT) before and after irradiation. The results indicate an increase in the extinction coefficient as a result of laser treatment with pulse laser with energy of 350 mJ, due to the increased absorbance of the P3HT polymer, as shown by the previous values. A significant similarity is evident between the curves of both the absorption coefficient and the extinction coefficient, due to the direct relationship between them. Microscopic defects are considered a major factor contributing to the increase in the extinction coefficient, as the scattering of incident photons can enhance the absorption of P3HT by organic molecules, in addition to the decomposition of structural defects in the polymer.

4.4 Dielectric properties

Both the real and imaginary parts of the samples' dependency on photon wavelength are shown in Figure 8 and Figure 9 respectively. The permittivity, often known as the dielectric constant, is a substantial dielectric property that affects the material's properties **[24-25]**. Dielectric susceptibility, wave impedance, relaxation duration, polarisability, molecular radius, specific and molar refraction, and polarisability are additional variables that are connected to this.

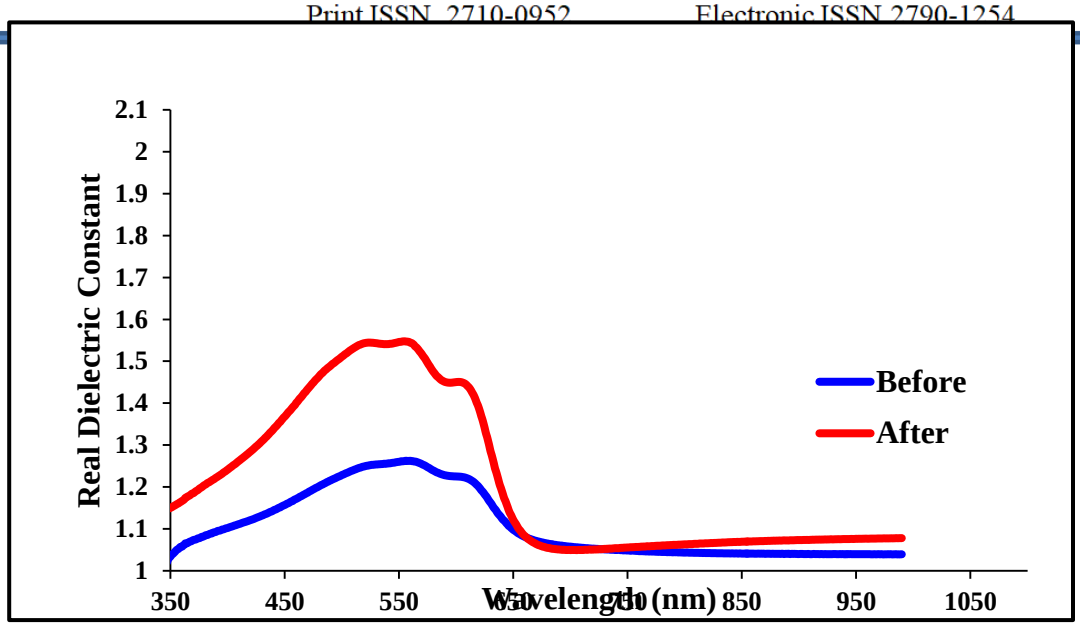

Figure 8. The real part of dielectric constant ε_r of P3HT film and for another P3HT thin irradiation with pulsed laser beams of energy (350 mJ).

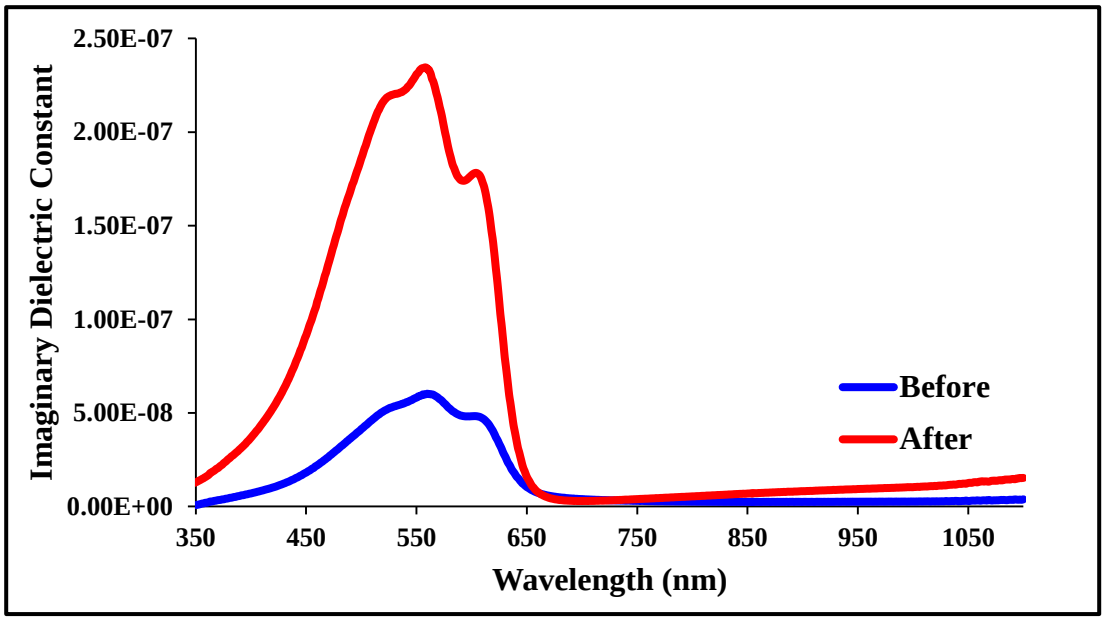

Figure 9. The imaginary part of dielectric constant of P3HT film and for another P3HT thin irradiation with pulsed laser beams of energy (350 mJ).

The complex dielectric constant is described by Equation 3:

$$\varepsilon = \varepsilon_r + i\varepsilon_i \quad \text{.....(3)}$$

in where (r) and (i) represent the real and imaginary parts of the dielectric constant, respectively. For the dielectric constant, the imaginary and real parts are given by equations 4 and 5, respectively:

$$\varepsilon_r = n^2 - k^2 \quad \text{.....(4)}$$

and

$$\varepsilon_i = 2nk \quad \text{.....(5)}$$

The real part of the dielectric constant is used to assess dispersion, while the imaginary part is used to measure the wave dissipative rate in the medium. Pulse laser treatment clearly shows that normal dispersion in the P3HT thin film increases the actual part of the dielectric constant εr. Additionally, it is presumed that εr is larger than εi since (r) is mostly dependent on n^2. Figure 8 and 9 show the peak, which represents the region of resonant absorption of the P3HT that was employed.

4.5 band gap energy

The optical energy gap (Eg) of P3HT films is shown in Figure 10 below. Due to its importance in the design and development of these organic materials, Eg is another fundamental parameter that characterizes semiconductors and dielectric materials.

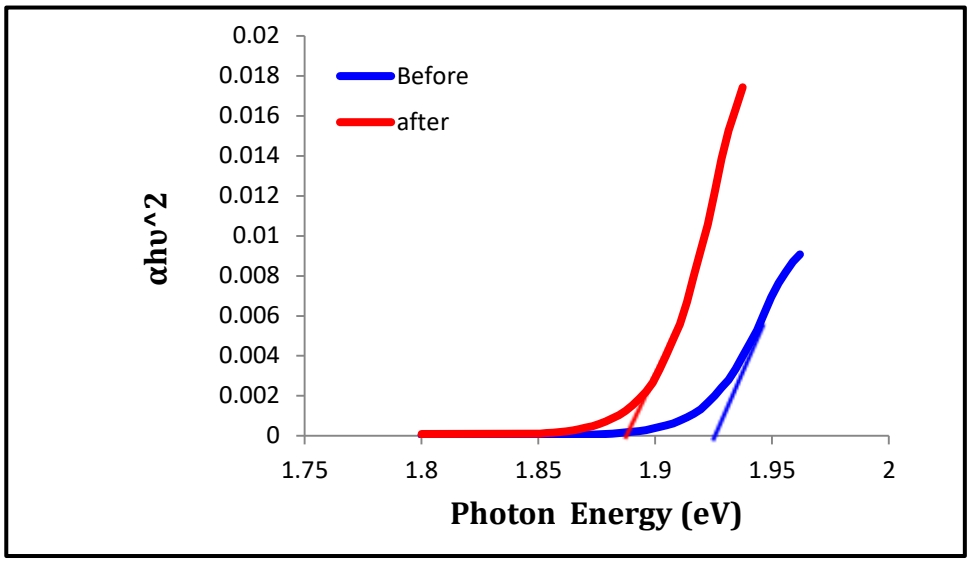

Figure 10. The energy gap of P3HT film and for another P3HT thin irradiation with pulsed laser beams of energy (350 mJ).

The optical energy gap of the samples was found by taking the intercept of the extrapolated linear component of the plot of $(\alpha h\upsilon)^2$ with the photon energy. The samples' band gap energies clearly dropped from 1.925 to 1.88 eV after pulse

laser treatment. Another reason for this is an increase in C-H bonds and C=H groups in the samples after laser treatment. It should be mentioned that the band gap is a significant consideration when selecting materials for various organic semiconductor applications [26]. In addition, lattice disorders and structural defects may be introduced during laser irradiation, leading to interstitial states between the HOMO and LUMO bands and so reducing the energy gap [17].

4.6 Infrared spectroscopy (FTIR)

The effects of laser irradiation on the molecular structures of P3HT thin films were investigated using the FTIR technique [27]. Figure 11 shows the infrared (IR) transmittance spectra of P3HT thin films before and after laser treatment with a pulse laser with energy of 350 mJ.

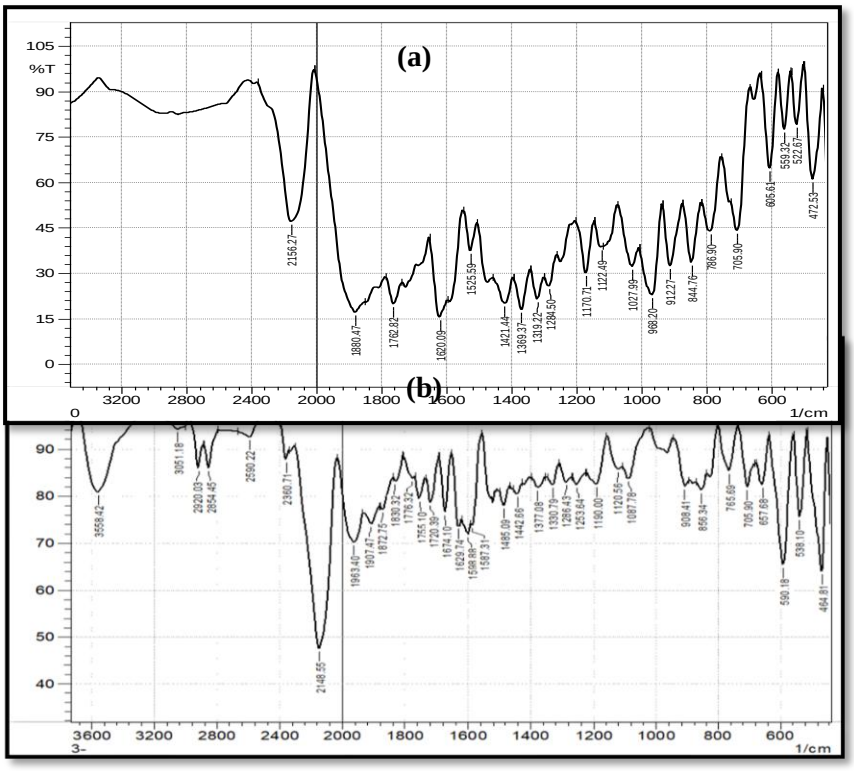

Figure 11. Illustrates the infrared transmittance spectra of P3HT thin films, both (a) before to and (b) following treatment with a pulse laser with an energy of 350 mJ.

The molecular bonds of P3HT IR spectra are concentrated in two areas before laser treatment: one around the wave numbers starting from 480 to 1880 cm^{-1}, and the other around the wave numbers 2158 cm^{-1}. This is shown in figure 11(a). The C-S stretching vibration is indicated by a weak band in the 600-700 cm^{-1} range, whereas the strong C-H bend is shown by the 650-1000 cm^{-1} range. In addition, the 1225-1025 cm^{-1} range is where the C=S bond's stretching frequency falls. Lastly, C=C medium stretch is denoted by 1680-1640 cm^{-1} and C-C medium stretch is 1500-1400 cm^{-1}. The C≡C weak stretch is clearly seen

in the second section. However, peaks at 2590.2, 2854.4, 2920 and 3051.1 cm^{-1} were seen after laser treatment utilizing a pulse laser with an energy of 350 mJ as shown in figure 11(b), which is due to the vibration of the C-H and =C-H bonds in the aliphatic chain of hexyl groups. The peak intensity is relatively high because the polymer has a high concentration of carbon-hydrogen bonds **[28]**.

4.7 X-ray diffraction (XRD)

To determine the chemical and crystal structures of P3HT, including its d spacing, crystallite size, lattice constants or parameters, and full width at half maximum (FWHM), x-ray diffraction is the most important instrument to utilize in this case. Characterization of P3HT organic thin films can reveal their chemical structure, crystal structure, and other properties. Such information is especially valuable for assessing the intermolecular interactions between adjacent molecules **[29].** As subsequently, the electrical behavior is greatly affected by the subsequent interactions between molecules,, which encompass the stacking of π-π molecules **[30]**. Figure 12 shows the XRD spectrum of the P3HT thin film before irradiation. Two diffraction peaks, at 2θ = 23.14 and 31.24, are clearly the most noticeable. By calculating their high-intensity full width at half maximum (FWHM), crystallite sizes may be found using equation 6 below that called the Scherrer equation:

$$D = \frac{k\,\lambda}{B\cos\theta} \quad \text{.....(6)}$$

In this equation, D indicates crystallite size, k is the form factor (0.9), λ is the X-ray wavelength (0.154 nm), β is the full width at half maximum (FWHM), and θ is the Bragg angle. The data utilized to determine the size of the crystallites is shown in Table 1.

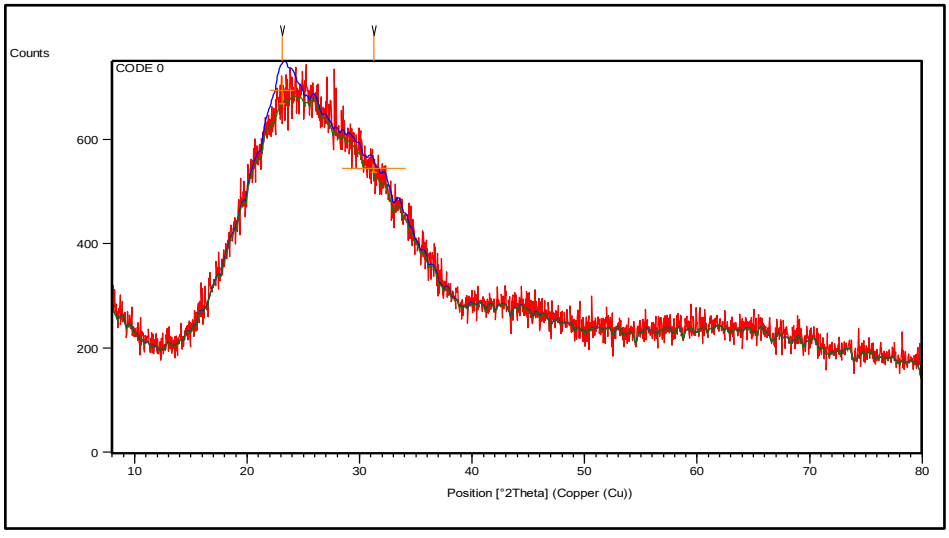

Figure 12.

Demonstrates the Diffraction peaks for P3HT film before pulse laser treatment.

Table 1: XRD peak list and structural characteristics for P3HT film before pulse laser treatment.

Pos. [°2Th.]	Height [cts]	FWHM Left [°2Th.]	d-spacing [A^0]	Rel. Int. [%]
23.1445	51.51	2.2042	3.84309	100.00
31.2477	15.11	5.6678	2.86252	29.32

In Figure 13, it can be seen the XRD spectrum of the irradiated P3HT thin film using a pulse laser with an energy of 350 mJ. The peak at 2θ=23.95 is clearly the most significant diffraction peak. Table 2 can be used once more to calculate the size of crystallites.

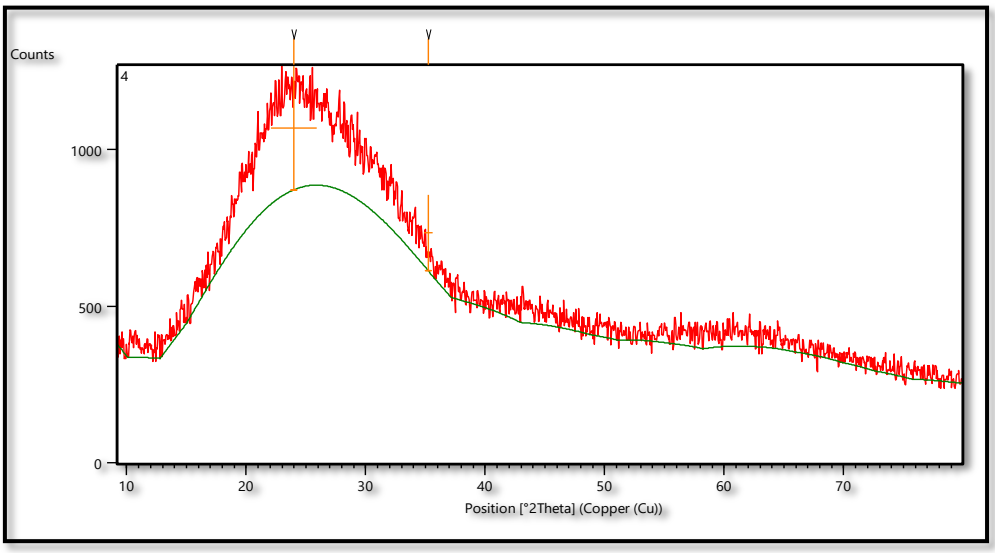

Figure 13. The Diffraction peaks for P3HT film after pulse laser treatment.

Table 2: Table 1: XRD peak list and structural characteristics for P3HT film after pulse laser treatment.

Pos. [°2Th.]	Height [cts]	FWHM Left [°2Th.]	d-spacing [Å]	Rel. Int. [%]	Tip Width
23.9589	395.65	3.8400	3.71120	100.00	4.6080
35.2319	242.38	0.6925	2.54741	61.26	0.8310

Figures 12 and 13 clearly show that the XRD spectrum showed the appearance of a new diffraction peak. What gives rise to the new peak spectrum is the spatial diversity in density inside the polymerized volume [32]. Samples irradiated to pulse laser treatment demonstrate a peak shift towards higher angles. It is possible to see the phase transition in these samples as leading to a general decrease in lattice constants and a contraction of the unit cells simultaneously [33]. Furthermore, before to laser treatments, the distance (d-space) between the atomic planes that generate diffraction peaks was 3.843A^{o}, and after pulse laser treatments, it decreased to 3.711A^{o}. This change in d-spacing and crystal size can be explained by the energy absorbed during processing. This energy directly breaks the molecular bonds within the material, causing material removal via molecular fragmentation without significant thermal damage, as a result of the dynamic interaction between the laser and the material. Here, equation 6 was used to calculate that the size of the crystallites was 1.004 nm after pulse laser treatment, down from 3.84 nm previously. As a consequence of laser-material interaction, the material's molecular chains may experience direct bond breaking, which may be attributed to changes in crystal size and d-spacing caused by the incident energy. Molecular fragmentation allows for material removal with minimal heat damage **[34].**

4.8 Atomic Force Microscope (AFM)

Atomic Force Microscope (AFM) analyses were performed on the P3HT samples before and after irradiation with pulsed laser beams of energy (350 mJ) to determine their morphology and surface roughness. Figure 14 presents two and three -dimensional AFM images of P3HT thin films, both in their as-deposited state and after pulse laser treatment.

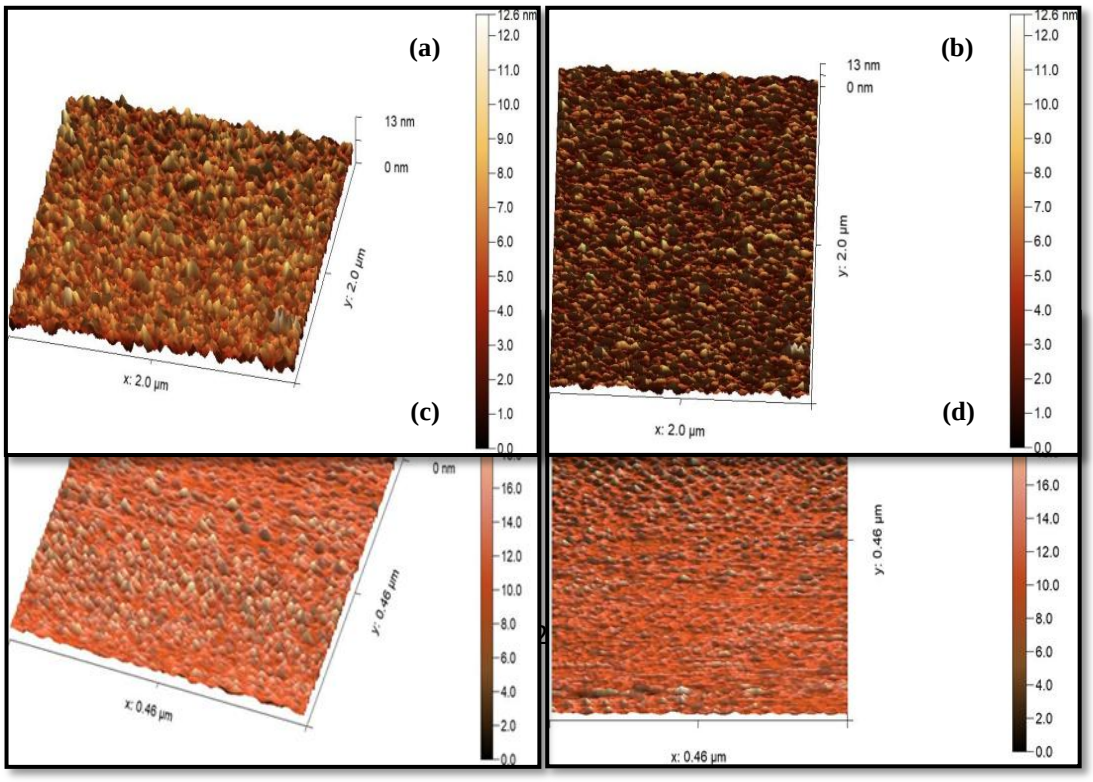

Figure 14. AFM images of P3HT thin films at (a, b) as-deposited thin film in three and two -dimensional respectively, (c, d) after laser treatment in three and two -dimensional respectively.

It can observed that ,the mean roughness of 1.1983 and a roughness mean square (rms) of 1.4630 nm characterize the morphology of the as-deposited P3HT film, which is characterized by a large number of grains and a tiny size. After pulse laser treatment with energy of 350 mJ, the P3HT film showed a roughness mean square of approximately 2.426 nm, while the average roughness increased to 1.863 nm. The change in grain size compared to the film before treatment indicates a shift in the degree of crystalline and self-organization within the polymer structure. It is noteworthy that no morphological changes occur on the polymer surface without external influence, and the roughness remains constant. Upon irradiated to high-energy pulsed lasers, however, the surface modification begins, as evidenced by the increase in roughness. Furthermore, structures begin to form in the form of clearly defined, parallel ripples within a narrow range of influences. This trend applies to most polymers, and this is consistent with what was obtained by Rebollar [35].

Conclusions

This study focus on how organic thin films of P3HT were affected by pulse laser treatment in terms of their crystalline structure and optical characteristics. Irradiated samples showed an increase in absorbance spectra after laser pulse treatment because the organic material's thin films had their molecular chains directly broken. The value of the absorption coefficient also increases due to pulse laser treatment. It was clear that band gap energy of the irradiated samples decreased using pulse laser treatment **with an energy of 350 mJ**. Additionally, the study looked at how laser irradiation changed the refractive index and real-imaginary dielectric constant. Clearly, there has been progress in both the real and fictional aspects. It is caused by an increase in the absorption coefficient. Thin films exposed to P3HT show fingerprint infrared peaks over the spectrum and several peaks at different places, according to the Fourier transform infrared spectroscopy (FTIR) technique. Overlapping aromatic C-H vibrations with CH-C-CH, C-C, and C-S vibrations, respectively, cause these peaks. A prominent peak going towards higher angles is observed in the XRD spectrum of irradiated materials after laser treatment. In these samples, the contraction of the unit cells and a general drop in lattice constants are both brought about by the phase transition. At last, the AFM showed that the P3HT's mean roughness and roughness mean square (rms) both increase following pulse laser treatment.

References:

[1] Morab, S., Sundaram, M. M., & Pivrikas, A. (2023). Review on charge carrier transport in inorganic and organic semiconductors. Coatings, 13(9), 1657.

[2] Manikantan, N. A., & Sathya, P.(2024) Organic Semiconductors: Exploring Principles and Advancements in OPV and OLED-A International Journal of Electrical and Electronics Engineering, 11(5), 60-76.

[3] Diesing, S., Zhang, L., Zysman-Colman, E., & Samuel, I. D. W. (2024). A figure of merit for efficiency roll-off in TADF-based organic LEDs. Nature, 627(8005), 747-753.

[4] Stingelin, N., Jurchescu, O. D., Wakayama, Y., & Orgiu, E. (2023). Next-Generation Organic Semiconductors–Materials, Fundamentals, and Applications. Advanced Materials Interfaces, 10(19).

[5] Jin, H., Kim, K., Kim, K., Park, S., Shin, E. Y., Heo, J. W., ... & Son, H. J. (2024). Development of degradable networked-organic semiconductors and effects on charge carrier mobility in organic thin-film transistors. Journal of Materials Chemistry C.

[6] Kim, K., Yoo, H., & Lee, E. K. (2022). New opportunities for organic semiconducting polymers in biomedical applications. Polymers, 14(14), 2960.

[7] Chen, X., Wang, Z., Qi, J., Hu, Y., Huang, Y., Sun, S., ... & Hu, W. (2022). Balancing the film strain of organic semiconductors for ultrastable organic transistors with a five-year lifetime. Nature Communications, 13(1), 1480.

[8] Yumusak, C., Sariciftci, N. S., & Irimia-Vladu, M. (2020). Purity of organic semiconductors as a key factor for the performance of organic electronic devices. Materials Chemistry Frontiers, 4(12), 3678-3689.

[9] Sawatzki-Park, M., Wang, S. J., Kleemann, H., & Leo, K. (2023). Highly ordered small molecule organic semiconductor thin-films enabling complex, high-performance multi-junction devices. Chemical Reviews, 123(13), 8232-8250.

[10] Poriel, C., & Rault-Berthelot, J. (2023). Dihydroindenofluorenes as building units in organic semiconductors for organic electronics. Chemical Society Reviews.

[11] Bertrandie, J., Han, J., De Castro, C. S., Yengel, E., Gorenflot, J., Anthopoulos, T., ... & Baran, D. (2022). The energy level conundrum of organic semiconductors in solar cells. Advanced Materials, 34(35), 2202575.

[12] Yang, X., & Ding, L. (2021). Organic semiconductors: commercialization and market. J. Semicond, 42(9), 090201.

[13] Pancaldi, A., Raimondo, L., Minotto, A., & Sassella, A. (2023). Post-growth dynamics and growth modeling of organic semiconductor thin films. Langmuir, 39(9), 3266-3272.

[14] Pope, T., Giret, Y., Fsadni, M., Docampo, P., Groves, C., & Penfold, T. J. (2023). Modelling the effect of dipole ordering on charge-carrier mobility in organic semiconductors. Organic Electronics, 115, 106760.

[15] Charoughchi, S., Liu, J. T., Berteau-Rainville, M., Hase, H., Askari, M. S., Bhagat, S., ... & Salzmann, I. (2023). Sterically-Hindered Molecular p-Dopants Promote Integer Charge Transfer in Organic Semiconductors. Angewandte Chemie, 135(31), e202304964.

[16] Suresh, D. S., Vandana, M., Veeresh, S., Ganesh, H., Nagaraju, Y. S., Vijeth, H., ... & Devendrappa, H. (2022,). Low Cost Synthesis and Characterization of Donor P3HT Polymer for Fabrication of Organic Solar Cell. In IOP Conference Series: Materials Science and Engineering (Vol. 1221, No. 1, p. 012060). IOP Publishing.

[17] Hussein, A. A., Sultan, A. A., Obeid, M. T., Abdulnabi, A. T., & Ali, M. T. (2015). Synthesis and Characterization of poly (3-hexylthiophene). International Journal of Scientific Engineering and Applied Science (IJSEAS)-Volume-1, Issue-7.

[18] Zakaria, N. A., & Malik, S. A. (2023). The influence of spin coating speed on the optical properties of P3HT thin film. In Journal of Physics: Conference Series (Vol. 2582, No. 1, p. 012027). IOP Publishing.

[19] Jarząbek, B., Nitschke, P., Godzierz, M., Palewicz, M., Piasecki, T., & Gotszalk, T. P. (2022). Thermo-optical and structural studies of iodine-doped polymer: Fullerene blend films, used in photovoltaic structures. Polymers, 14(5), 858.

[20] Miled, A., Saidi, H., Dhifaoui, H., Hannachi, R., & Bouazizi, A. (2022). Electro-optical properties improvement of organic composite using p-nitro-benzylidenemalonotrile-based small organic molecules. Bulletin of Materials

Science, 45(3), 113.

[21] Wangui, E., Ikua, B. W., & Nyakoe, G. N. (2022, June). A study on influence of beam orientation in engraving using CO2 laser. In Proceedings of the Sustainable Research and Innovation Conference (pp. 126-131).

[22] Zahedi, S., & Dorranian, D. (2013). Effect of laser treatment on the optical properties of poly (methyl methacrylate) thin films. Optical review, 20, 36-40.

[23] Liu, J., Wang, C., Dang, Z., Chu, Y., & Zhang, Z. (2022). Thermally resettable laser transmission induced transparency in polymer waveguides at 635 nm. Optics Express, 30(10), 17529-17540.

[24] Torshkhoyeva, Z. S., Kunizhev, B. I., & Kharaev, A. M. (2023). The Investigation of the effect of laser radiation on the dielectric properties of polymethylmethacrylate. In E3S Web of Conferences (Vol. 413, p. 02039). EDP Sciences.

[25] Yang, X., Liu, J., & Koster, L. J. A. (2024). The Exceptionally High Dielectric Constant of Doped Organic Semiconductors. Advanced Electronic Materials, 2400413.

[26] Saqib, M., Rani, M., Mubashir, T., Tahir, M. H., Maryam, M., Mushtaq, A.,.. & Elansary, H. O. (2024). Designing of low band gap organic semiconductors through data mining from multiple databases and machine learning assisted property prediction. Optical Materials, 150, 115295.

[27] Khan, S. A., Khan, S. B., Khan, L. U., Farooq, A., Akhtar, K., & Asiri, A. M. (2018). Fourier transform infrared spectroscopy: fundamentals and application in functional groups and nanomaterials characterization. Handbook of materials characterization, 317-344.

[28] Rao, C. N. R., Venkataraghavan, R., & Kasturi, T. R. (1964). Contribution to the infrared spectra of organosulphur compounds. Canadian journal of chemistry, 42(1), 36-42.

[29] Schweicher, G., Das, S., Resel, R., & Geerts, Y. (2024). On the importance of crystal structures for organic thin film transistors. Crystal Structure Communications, 80(10).

[30] McHugh, C. J. (2024). Crystal clear: the impact of crystal structure in the

development of high-performance organic semiconductors. Crystal Structure Communications, 80(11), 696-697.

[31] Astuti, B., Zhafirah, A., Carieta, V. A., Hamid, N., Marwoto, P., Nurbaiti, U., ... & Aryanto, D. (2020, June). X-ray diffraction studies of ZnO: Cu thin films prepared using sol-gel method. In Journal of Physics: Conference Series (Vol. 1567, No. 2, p. 022004). IOP Publishing.

[32] Klein, S., Crégut, O., Gindre, D., Boeglin, A., & Dorkenoo, K. D. (2005). Random laser action in organic film during the photopolymerization process. Optics Express, 13(14), 5387-5392.

[33] Mostafa, M., Ebnalwaled, K., Saied, H. A., Roshdy, R., Mostafa, M., Ebnalwaled, K., ... & Roshdy, R. (2018). Effect of laser beam on structural, optical, and electrical properties of BaTiO 3 nanoparticles during sol-gel preparation. Journal of the Korean Ceramic Society, 55(6), 581-589.

[34] Wangui, E., Ikua, B. W., & Nyakoe, G. N. (2022, June). A study on influence of beam orientation in engraving using CO2 laser. In Proceedings of the Sustainable Research and Innovation Conference (pp. 126-131).

[35] Rebollar, E., Castillejo, M., & Ezquerra, T. A. (2015). Laser induced periodic surface structures on polymer films: From fundamentals to applications. European Polymer Journal, 73, 162-174.